Detailed Mechanistic Studies using *in situ* Spectroscopic Analysis: A Look at Little-Known Regions of the Heck Reaction

Gadi Rothenberg,* Susana C. Cruz, Gino P. F. van Strijdonck, Huub C. J. Hoefsloot

van't Hoff Institute for Molecular Sciences, University of Amsterdam, Nieuwe Achtergracht 166, 1018 WV Amsterdam, The Netherlands
Fax: (+31)-20-525-5604, e-mail: gadi@science.uva.nl

Received: October 8, 2003; Accepted: January 21, 2004

Abstract: The mechanism of the Heck reaction using palladium complexes with large phosphoramidite ligands is investigated. The catalyst precursor is an inactive dimer that equilibrates with the active monomeric species. A series of kinetic models is introduced and compared with concentration profiles obtained from FT-NIR spectroscopy. First, an analytical solution of the differential equations for a simplified mechanism is considered. This fits well at low conversions but deviates at higher conversions with increasing deactivation. Formation of palladium clusters and palladium black is then included, with the simplification that all the deactivation processes are represented by a single first-order process. This results in a five-step mechanism that describes the dimer-monomer equilibrium, the Pd(II)/Pd(0) catalytic cycle, and the catalyst deactivation process. The model can be used to monitor the transient concentrations of the virtual Pd(0), Pd(II), and dimer catalyst species, and helps to explain the effects of water. The high resolution of the measurements and low error levels of the models render this approach a powerful tool for mechanistic studies in homogeneous catalysis.

Keywords: catalyst deactivation; cross coupling; homogeneous catalysis; kinetic analysis; palladium; spectroscopy

Introduction

The palladium-catalysed cross-coupling of aryl halides and olefins (the Heck reaction) is one of the most useful protocols in fine-chemical synthesis.[1–6] The reaction tolerates a broad range of functional groups and conditions, and has been optimised to give turnover numbers and turnover frequencies in the millions.[7,8] It is also used in several large-scale commercial processes.[9,10] Hundreds of studies were published on this reaction since its discovery by Heck and Mizoroki in 1968, but the intricate mechanism of the catalytic cycle is still a hot point of scientific debate, that also extends to the mechanisms of the Stille, Suzuki, and Ullmann coupling reactions.[11–15] The classic four-step catalytic cycle (Scheme 1) is riddled with solvent,[16] salt,[17–19] and catalyst precursor[20] side-effects that, contrary to their name, are now considered to play a major role in the reaction. Another problem is the deactivation of the homogeneous palladium catalyst *via* clustering to form palladium black.[21] The palladium clusters complicate things even further, as they themselves may catalyse the reaction or act as catalyst precursors.[22,23]

A promising ligand system for the Heck reaction is the family of bulky monodentate phosphoramidites.[24]

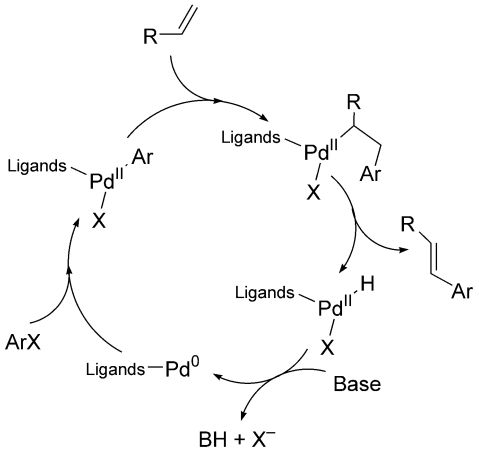

Scheme 1. Classic catalytic cycle for the Heck reaction.

Here the catalyst precursor is a dimer. Although the isolated dimer **1** is itself inactive, when dissolved in the reaction mixture it equilibrates with the monomer **2**, that can then participate in the catalytic cycle (Scheme 2). Dimer-monomer catalyst equilibria are reported for a number of palladium-catalysed reactions, and recent investigations support the concept where the

 DOI: 10.1002/adsc.200303163

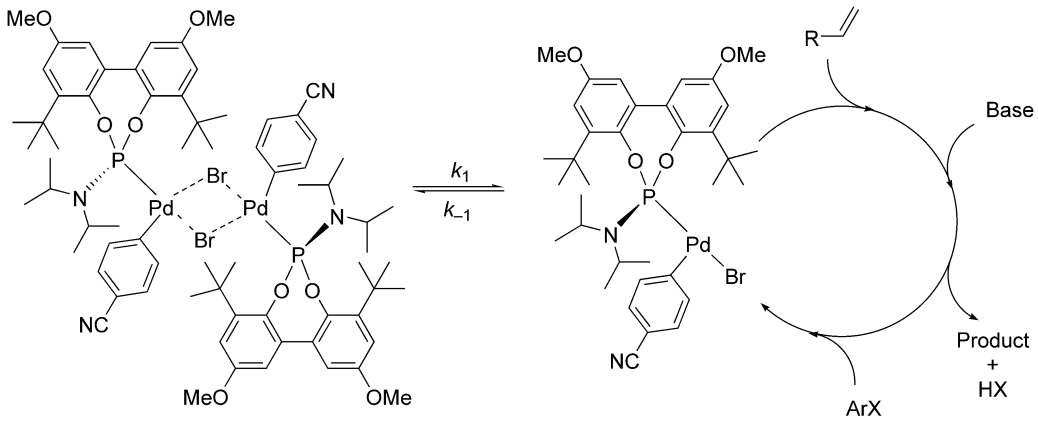

Scheme 2. Dimer-monomer equilibrium and catalytic cycle. Note that in the first turnover the Heck product will be dictated by the organic residue of the catalyst precursor, in this case PhCN. In subsequent turnovers the product will depend on the ArX substrate.

dimer acts as a 'reservoir' for the active monomer.[25,26] However, as in many homogeneously catalysed systems, it is difficult to propose a comprehensive mechanism due to the complexity of the reaction and the lack of high-resolution concentration profiles.

In this paper, we monitor the Heck reaction between PhI and *n*-butyl acrylate to give *n*-butyl cinnamate in the presence of the dimer catalyst precursor **1**. Using *in situ* high resolution near-infrared spectroscopy, we examine the reaction profiles in detail and fit a kinetic model to the data. To our knowledge, this is the first model that explains all three stages of the reaction: the dimer-monomer equilibrium activation period, the catalytic cycle itself, and the deactivation of the catalyst as palladium black.

Results and Discussion

In a typical reaction [Eq (1)], PhI, *n*-butyl acrylate, and Et_3N were mixed in *N*-methylpyrrolidone (NMP) in the presence of 1.0 mol % dimer **1** at 50 °C. The concentration profiles of PhI and *n*-butyl cinnamate were monitored using Fourier-transform near-infrared (FT-NIR) spectroscopy. For comparison and validation purposes, samples were also analysed by GC.

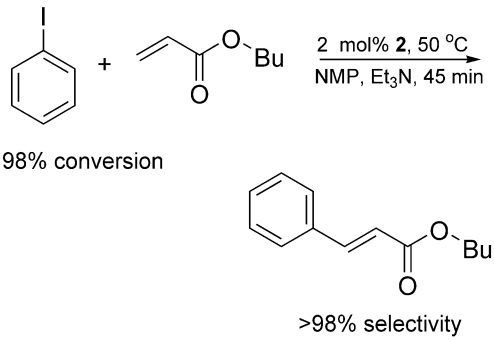

(1)

Previously, based on preliminary kinetic profiles at 80 °C obtained using GC analysis, one of us proposed a first-order mechanism for this reaction, with the migratory insertion as the rate-determining step.[24] This simplified mechanism does not take into account the full dimer-monomer equilibrium and the fact that the homogeneous Pd(0) complex deactivates as palladium black. However, the mechanism is in good agreement with the GC data at low and medium substrate conversions.

By lowering the reaction temperature to 40 – 50 °C and using FT-NIR, we can probe the mechanism in detail. In contrast to GC, FT-NIR affords an excellent time resolution, which means that every reaction profile contains sufficient sample points to enable a meaningful residuals analysis. Moreover, precise monitoring of the reactants and products over the entire reaction duration enables the construction of kinetic models that take into account the whole reaction profile, giving a more accurate presentation than the conventional initial rate methods.[26] Figure 1 shows a typical concentration profile of PhI obtained at 50 °C (for comparison, the results of the GC analysis are also shown). The profile is more complex than a first-order reaction. It begins with an activation period, and ends with a deactivation (the formation of palladium black). Furthermore, it shows a curious acceleration in between (*vide infra*). Nevertheless, the first-order rate constant estimated from this profile can still be used as a starting guess for the more detailed kinetic and mechanistic models.

The kinetic model was constructed in two stages. First, we extended the mechanism to include the dimer-monomer equilibrium [Eqs. (2) and (3), where k_1 and k_2 are the rate constants for the dissociation and the formation of the dimer precursor, and k_3 is the rate constant for the catalytic reaction).

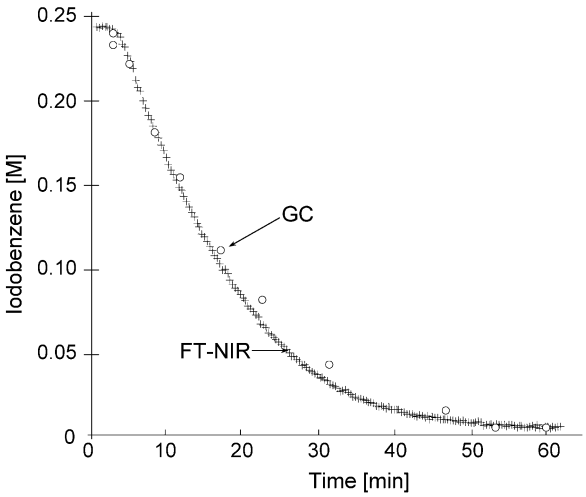

Figure 1. Time-resolved reaction profiles for iodobenzene conversion in the Heck coupling with butyl acrylate at 50 °C; '+' symbols represent FT-NIR data; '○' symbols represent GC data from the same reaction.

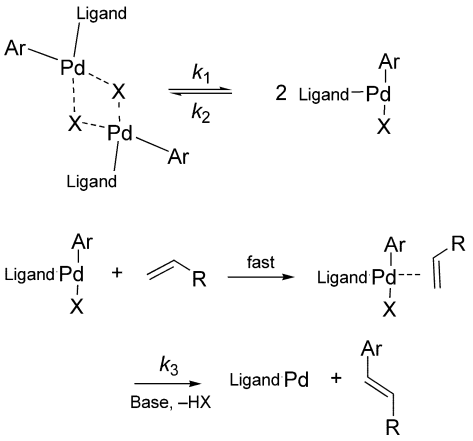

(2)

(3)

If we then denote the dimer as A, the monomer as Q, and the aryl halide as B, we obtain the simple pair of equations (4) and (5), from which we derive the corresponding pair of differential equations (6) and (7).

Rather surprisingly, these differential equations do have an analytical solution [Eqs (8) and (9), respectively, where $A(0) = A_0$ and $B(0) = B_0$]. This solution describes a process that begins with an induction period, followed by a reaction that obeys a first-order rate law in the palladium concentration. The induction period ends when the dimer-monomer equilibrium is reached. Using this analytical solution, we can generate simulated concentration profiles that correspond to various $\{k_1, k_2, k_3\}$ sets, and superimpose these on the experimental results. The set $\{k_1 = 0.0746,\ k_2 = 6.07,\ k_3 = 17.46\}$, obtained by a least-squares fit of Eqs. (8) and (9) to the experimental reaction profile at 40 °C, explains well the experimental results, including the initial induction period (see Figure 2). The length of the induction period strongly depends on the temperature and on the magnitudes of k_1, k_2, and k_3. The ratio k_2/k_1 equals 81.3, which corresponds to an equilibrium constant for the dimer dissociation $K_{diss} = 0.012$ M. Although the

$$A \underset{k_2}{\overset{k_1}{\rightleftharpoons}} 2Q \tag{4}$$

$$Q + B \xrightarrow{k_3} Q + \text{Product} \tag{5}$$

$$\frac{dA(t)}{dt} = -k_1 A(t) + 4\,k_2 \left(A_0 - A(t)\right)^2 \tag{6}$$

$$\frac{dB(t)}{dt} = -2\,k_3 \left(A_0 - A(t)\right) B(t) \tag{7}$$

$$2Q^0 \underset{}{\overset{k_{d1}}{\rightleftharpoons}} (Q^0)_2 \tag{10}$$

$$Q + Q^0 \underset{}{\overset{k_{d2}}{\rightleftharpoons}} QQ^0 \tag{11}$$

$$(Q^0)_2 + Q \xrightarrow{k_{d3}} Q(Q^0)_2 \tag{12}$$

$$QQ^0 + Q \xrightarrow{k_{d4}} QQ^0Q \tag{13}$$

$$(Q^0)_2 + Q^0 \xrightarrow{k_{d5}} (Q^0)_3 \text{ or } Q^0(Q^0)_2 \tag{14}$$

$$QQ^0 + Q^0 \xrightarrow{k_{d6}} QQ^0Q^0 \quad \textit{... et cetera} \tag{15}$$

$$A(t) = \frac{1}{8\,k_2}\left(k_1 + 8\,A_0 k_2 - \sqrt{k_1\left(k_1 + 16\,A_0 k_2\right)}\,\tanh\left[\frac{1}{2}\sqrt{k_1\left(k_1 + 16\,A_0 k_2\right)}\,t + \operatorname{arctanh}\left[\frac{k_1}{\sqrt{k_1\left(k_1 + 16\,A_0 k_2\right)}}\right]\right]\right) \tag{8}$$

$$B(t) = 2^{\frac{k_3}{k_2}} B_0 e^{\frac{k_1 k_3 t}{4k_2}} \left(\frac{A_0 k_2}{k_1 + 16 A_0 k_2}\right)^{\frac{k_3}{4k_2}} \cosh\left[\frac{1}{2}\sqrt{k_1\left(k_1 + 16\,A_0 k_2\right)}\,t + \operatorname{arctanh}\left[\frac{k_1}{\sqrt{k_1\left(k_1 + 16\,A_0 k_2\right)}}\right]\right]^{\frac{k_3}{2k_2}} \tag{9}$$

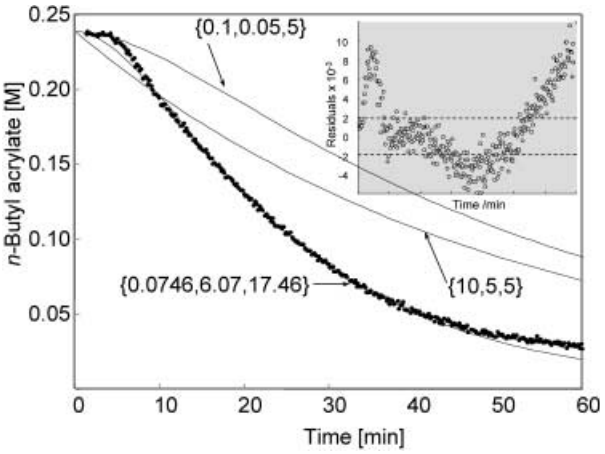

Figure 2. Three reaction profiles generated from the analytical solution shown in Eqs. (8) and (9) (solid curves). Each curve corresponds to a set of $\{k_1, k_2, k_3\}$ values. The results are compared to the FT-NIR data (dotted curve, obtained at 40 °C). The inset shows the residuals obtained when the solution for the set $\{k_1 = 0.0746,\ k_2 = 6.07,\ k_3 = 17.46\}$ is superimposed on the FT-NIR data, the dashed lines in the inset denote the experimental error limits.

model is still inaccurate because no deactivation is included, this low equilibrium constant already shows that most of the catalyst is present as the inactive dimer.

The residuals, however, are still structured (see inset in Figure 2), even at low conversions where deactivation is supposed to play only a minor role. This is not surprising, as the large number of data points gives a precise representation of the reaction profile, and in reality deactivation through clustering begins as soon as there are Pd(0) species in the solution (in all of the reactions, palladium black formed at 20–50% conversion). Moreover, as the model tries to describe all of the data, deviations at higher conversions will affect the model also in the beginning of the reaction. The deactivation increases with the conversion. At *ca.* 70% conversion, it becomes the dominant factor and the model deviates from the data. Nevertheless, the overall fit is remarkable, considering the simplicity of the model and the complexity of the reaction.

With the above model as a starting point, we considered possible pathways for catalyst deactivation.[21] In principle, whenever the palladium atoms cluster, chances are that they will not dissolve back into solution but aggregate further and finally precipitate from the solution as palladium black. In addition to the formation of Pd(0) clusters, disproportionation of {Pd(II), Pd(0)} pairs is also possible.[27] These various clusters can react further with Pd(0), Pd(II), and/or with any of the clusters already present in the solution. If we encode, as above, Pd(II) as Q, and Pd(0) as Q^0, we obtain a plethora of (reversible?) deactivation processes [Eqs (10)–(15)] for which there is obviously no analytical solution. Furthermore, even if one can fit the deactivation constants k_{d1} to k_{d6} using numeric methods, what would be the chemical meaning of such a complicated model? Instead, we chose to combine all of the deactivation reactions into one process, regardless of the palladium species that is deactivating. This simplification basically states that all palladium species can deactivate *via* a first-order process with a single deactivation constant.

Finally, we extended the model of the catalytic cycle to include the formation of a Pd(II) species and a Pd(0) species. The overall reaction mechanism is shown in Eqs. (16)–(18). The differential equations that correspond to Eqs. (16)–(18) have no analytical solution, but they can be solved numerically using an iterative process. Solving for the reaction rate constants $\{k_1 ... k_5\}$ we obtain the set {0.362, 289.8, 53.90, 14.00, 39.80}. k_1 is much smaller than k_2, meaning that the dimer dissociation is very slow. Once enough Q species form, the catalytic cycle and the deactivation proceed at similar rates. As shown in Figure 3, this solution gives an excellent fit to the experimental data, and yet it uses only five variables (five kinetic constants). Moreover, this mechanism tallies with 'chemical intuition' as well as with previous simpler models. The residuals are mostly

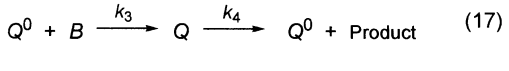

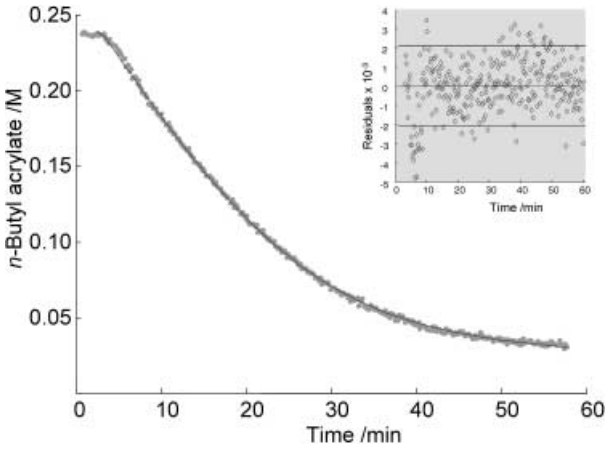

Figure 3. The solid curve is the reaction profile for the Heck coupling of *n*-butyl acrylate and iodobenzene generated from the numerical solution of the differential equations pertaining to the mechanism shown in Eqs. (16)–(18). Superimposed on this profile is the actual experimental data obtain by FT-NIR. Reaction conditions are as in Figure 2. The inset shows the residuals (dashed lines in the inset denote the experimental error limits).

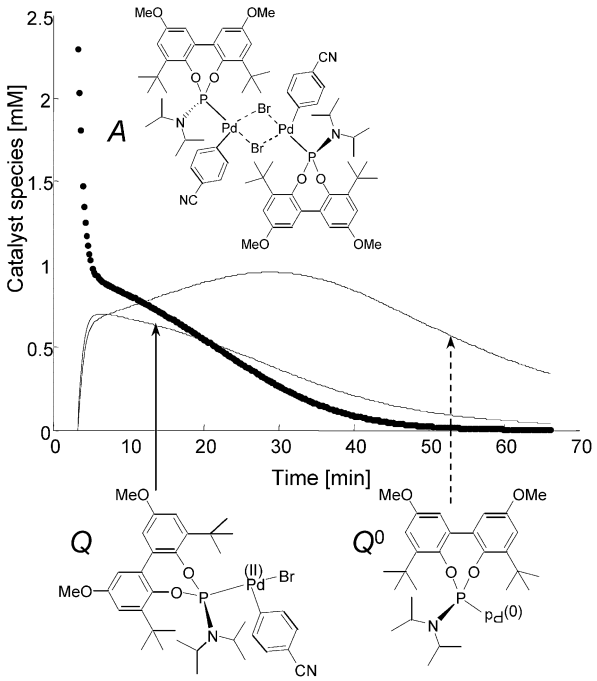

Figure 4. Calculated concentration profiles for the dimer species A ('●' symbols) and the two monomer species Q (solid curve) and Q^0 (broken curve) calculated from the numeric solution of the differential equations pertaining to the mechanism shown in Eqs. (16) – (18). Reaction conditions are as in Figure 2.

within the experimental error limits (Figure 3, inset). In the new model, the equilibrium constant for the dimer dissociation is only 1.2×10^{-3} M, giving further support to the hypothesis that most of the catalyst is present in solution as the inactive dimer.

In addition to providing values for the reaction and the deactivation rate constants, we can use this kinetic model to track virtual 'catalyst species' in time (there is often no way to do this experimentally, because it is difficult to monitor the low concentrations of similar species such as Q and Q^0 with any accuracy). Figure 4 shows the calculated reaction profiles for the dimer precursor and the two monomer species. We see that first the dimer concentration declines, and subsequently the concentrations of the Pd(II) and Pd(0) monomer species increase to a 'steady state' level, that gradually diminishes owing to the deactivation process. The deactivation also shifts the dimer-monomer equilibrium to the side of the active monomer. If we consider the 15 – 30 min range, we see that the deactivation even accelerates the reaction at first, as more and more Q^0 species are formed.

The generality of a model is a measure of its usefulness. If we make small changes to the system, we should expect these changes to be reflected in the values of $\{k_1...k_5\}$. The changes should be sufficiently small so that the reaction pathway itself is not altered. To test this, we performed more reactions, this time without filtering the water residues from the solvent. These small amounts of water are known to promote catalyst deactivation. A kinetic analysis of the concentration profile in the presence of water gave the k values {0.119, 288.2, 35.00, 11.90, 831.7}. Comparing these values with those obtained in the absence of water {0.362, 289.8, 53.90, 14.00, 39.80}, we see that the dimer-monomer equilibrium is almost unchanged, and that the values of k_3 and k_4 also remain very similar. The only major change is in the deactivation constant – it is twenty times higher in the presence of water! Again, the model is in good agreement with empirical findings.

Another interesting point is the difference between the first turnover and the subsequent ones. The dimer **1** is comprised of two monomers that already include an ArX molecule. In this study we used *p*-cyanobromobenzene to prepare **1**, as this gives a stable dimer (we have tried to use the corresponding PhI derivative, but it is much more difficult to isolate and store without decomposition). The dimer-monomer equilibrium is thus also a function of the reaction progress – immediately in the beginning of the reaction, all the catalysts would give the cyano derivative of the product, rather than product **2**. As more and more catalyst molecules react, the balance will change in favour of product **2** formed from iodobenzene. There is only 1 mol % catalyst, so the effect on the product yield is small. The effect on the initial kinetics of the reaction, however, is significant. The model cannot account for this discrepancy, as it does not distinguish between the two substrates. If we try to model it, it gives a biased result, but no bias is observed if we exclude the first 15 time points (out of 271). This means that it takes *ca.* 8 min to take the cyano 'pre-catalyst' out of the catalytic cycle.

Finally, one may ask whether these results can be generalised to other, similar cross-coupling reactions. Recently, Blackmond and co-workers have used calorimetry to monitor a Heck coupling reaction catalysed by a dimeric palladacycle complex.[20,26] In that system, the catalyst precursor is converted to the active monomer by a reduction step, which is assumed to be irreversible under the conditions employed. The rate law obtained for that system is complicated by this extra activation step and no deactivation is included, but the conclusion is essentially similar: Most of the catalyst exists in solution as the dimer that functions as a 'reservoir' for generating the monomer. This can help us in devising more efficient catalyst systems: A lower palladium concentration can assist the reaction kinetics, as the amount of active catalyst is limited by the dimer-monomer equilibria rather than determined by the overall palladium concentration. In principle, immobilisation of the palladium catalyst could help overcome the deactivation problem, enabling the system to operate also at higher palladium concentrations.

Conclusions

From initial rate kinetics carried out under pseudo-order conditions it may seem that palladium-catalysed Heck reactions are simple, but the simplified reaction schemes are to some extent a result of the measurement conditions themselves. In contrast, non-invasive *in situ* spectroscopic analysis is a powerful method for obtaining precise mechanistic information under actual reaction conditions. Using real-time FT-NIR, we show here that for the catalysts investigated in this study the dimer-monomer equilibrium governs the reaction's induction period, and that a mechanism with two 'virtual species' of Pd(0) and Pd(II) can fit the experimental data over the entire reaction duration to a series of well defined elementary reactions. The model is sufficiently robust to withstand changes in the experimental conditions, such as the presence/absence of water. The operational ease and the low computational costs of the models involved make this approach a powerful tool for mechanistic investigations in homogeneous catalysis.

Experimental Section

Near-infrared spectra were recorded on a Perkin Elmer Spectrum GX FT-IR instrument from 15000 cm^{-1} to 2700 cm^{-1} at 2 cm^{-1} resolution. Spectral data analysis was performed using the Net Analyte Signal (NAS) approach.[28,29] GC analysis was performed using an Interscience GC 8000 *Top* instrument with a DB-1 column (30 m × 0.32 mm; film thickness 3 μm). Unless noted otherwise, chemicals were purchased from commercial firms (> 98% pure) and used as received. The catalyst precursor **1** was synthesized as published previously.[24] *n*-Butyl acrylate was filtered prior to use through a plug of basic alumina (*ca.* 150 mesh size) to remove the quinone stabiliser. *N*-Methylpyrrolidinone (NMP, solvent) was also filtered prior to use, except in the water-containing experiments.

Procedure for Heck Coupling of PhI with *n*-Butyl Acrylate

PhI (1.16 mmol, 0.237 g), *n*-butyl acrylate (1.16 mmol, 0.149 g) and Et_3N (1.33 mmol, 0.135 g) were mixed in *N*-methylpyrrolidinone (2.5 mL) for 5 min at 40 ^{0}C together with an equimolar amount of dihexyl ether (internal standard for GC measurements). In another vial, the catalyst precursor dimer **1** (0.0131 mmol, 10.2 mg, 1.1 mol % relative to substrate) was dissolved in NMP (2.5 mL) and warmed to 40 ^{0}C. The two solutions were then mixed to start the reaction. The concentrations of *n*-butyl acrylate and PhI at t = 0 were 0.233 M and 0.256 M, respectively. The reaction mixture was divided into two vessels, an FT-NIR cuvette and a vessel for taking GC samples. Both vessels were kept under identical conditions using a thermoregulated bath. 10 μL aliquots of the reaction mixture were taken at regular intervals, quenched with a saturated NH_4Cl solution in H_2SO_4 0.05 M and analysed by GC. The reaction at 50 ^{0}C was similarly performed. Duplicate experiments showed excellent concentration reproducibility.

Kinetic Analysis

If a kinetic scheme and data are present it is possible to find estimates of the kinetic constants. One way to do this is to define a χ^2 merit function [Eq. (19)] and then determine the constants by minimising this merit function.[30]

$$\chi^2(\mathbf{k}) = \sum_{i=1}^{N} \left[y_i - \hat{y}_i(\mathbf{k}) \right]^2 \quad (19)$$

Here y_i are the measurements, $\hat{y}_i$ are the estimations from the model and **k** is the vector of unknown kinetic constants. We seek those values for **k** that give the lowest difference in square sense of the model with the measurements. There are several numerical options to perform this search. We used a MATLAB[31] standard non-linear least squares solver, LSQNONLIN. This method requires initial guesses of **k** to find a minimum. Care should be taken when assigning these initial values, as they can also lead to local minima of the merit function, rather than to the desired global minimum. To avoid these local minima, we fit first the kinetic constants using the simplified reaction scheme given in Eqs. (4) and (5) (no deactivation) to the first part of the data where catalyst deactivation is negligible. We then confirm that the results are independent of the initial guesses. Finally, we use these estimates together with an initial value for the deactivation rate constant k_5 as initial values for the whole set of data using the complex kinetics scheme [Eqs. (16) – (18), deactivation included]. This two-step procedure turned out to be robust against variations in the initial guesses and we therefore assume that the global minimum for the merit function has been reached. It is impossible to rigorously prove that the results are indeed at the global minimum. One diagnostic tool is to examine whether other initial guesses yield a lower minimum value. Another diagnostic tool is to study the residuals, *i.e.* the differences between measurement and model, as shown in Figures 2 and 3. Structure in these residuals would mean that either the model is not perfect (as we believe the case is here, using the simplified one-constant deactivation process) or that the minimisation algorithm is stuck in a local minimum.

References

[1] I. P. Beletskaya, A. V. Cheprakov, *Chem. Rev.* **2000**, *100*, 3009.
[2] J. McChesney, *Spec. Chem.* **1999**, *19*, 98.
[3] T.-C. Wu, V. Ramachandran, *Innovations Pharm. Technol.* **2000**, 97.
[4] T. Mizoroki, *Bull. Chem. Soc. Jpn.* **1971**, *44*, 581.
[5] W. A. Hermann, in: *Applied Homogeneous Catalysis with Organometallic Compounds,* Vol. 2, (Eds.: B. Cornils, W. A. Hermann), VCH, Weinheim, **1996**.
[6] R. F. Heck, J. P. Nolley, *J. Org. Chem.* **1972**, *37*, 2320.
[7] M. Ohff, A. Ohff, M. E. van der Boom, D. Milstein, *J. Am. Chem. Soc.* **1997**, *119*, 11687.

[8] M. Ohff, A. Ohff, D. Milstein, *Chem. Commun.* **1999**, 357.
[9] J. G. de Vries, *Can. J. Chem.* **2001**, *79*, 1086.
[10] H.-U. Blaser, A. Indolese, A. Schnyder, *Curr. Sci.* **2000**, *78*, 1336.
[11] G. T. Crisp, *Chem. Soc. Rev.* **1998**, *27*, 427.
[12] F. Diederich, P. J. Stang, *Metal-catalyzed Cross-coupling Reactions*, Wiley-VCH, Weinheim, **1997**.
[13] J. Louie, J. F. Hartwig, *Angew. Chem. Int. Ed. Engl.* **1996**, *35*, 2359.
[14] B. L. Shaw, S. D. Perera, *Chem. Commun.* **1998**, 1863.
[15] J. A. Loch, M. Albrecht, E. Peris, J. Mata, J. W. Faller, R. H. Crabtree, *Organometallics* **2002**, *21*, 700.
[16] W. Cabri, I. Candiani, S. DeBernardinis, F. Francalanci, S. Penco, R. Santo, *J. Org. Chem.* **1991**, *56*, 5796.
[17] C. Amatore, M. Azzabi, A. Jutand, *J. Am. Chem. Soc.* **1991**, *113*, 8375.
[18] C. Amatore, E. Carre, A. Jutand, M. A. M'Barki, G. Meyer, *Organometallics* **1995**, *14*, 5605.
[19] C. A. Merlic, M. F. Semmelhack, *J. Organomet. Chem.* **1990**, *391*, C23.
[20] T. Rosner, A. Pfaltz, D. G. Blackmond, *J. Am. Chem. Soc.* **2001**, *123*, 4621.
[21] P. W. N. M. van Leeuwen, *Appl. Catal. A: Gen.* **2001**, *212*, 61.
[22] M. T. Reetz, E. Westermann, *Angew. Chem. Int. Ed.* **2000**, *39*, 165.
[23] M. T. Reetz, R. Breinbauer, K. Wanninger, *Tetrahedron Lett.* **1996**, *37*, 4499.
[24] G. P. F. van Strijdonck, M. D. K. Boele, P. C. J. Kamer, J. G. de Vries, P. W. N. M. Van Leeuwen, *Eur. J. Inorg. Chem.* **1999**, 1073.
[25] W. A. Herrmann, C. Brossmer, K. Oefele, C.-P. Reisinger, T. Priermeier, M. Beller, H. Fischer, *Angew. Chem. Int. Ed. Engl.* **1995**, *34*, 1844.
[26] T. Rosner, J. Le Bars, A. Pfaltz, D. G. Blackmond, *J. Am. Chem. Soc.* **2001**, *123*, 1848.
[27] M. Tromp, J. R. A. Sietsma, J. A. van Bokhoven, G. P. F. van Strijdonck, R. J. van Haaren, A. M. J. van der Eerden, P. W. N. M. van Leeuwen, D. C. Koningsberger, *Chem. Commun.* **2003**, 128.
[28] A. Lorber, K. Faber, B. R. Kowalski, *Anal. Chem.* **1997**, *69*, 1620.
[29] S. C. Cruz, P. J. Aarnouste, G. Rothenberg, J. A. Westerhuis, A. K. Smilde, A. Bliek, *Phys. Chem. Chem. Phys.* **2003**, *5*, 4455.
[30] W. H. Press, B. P. Flannery, S. A. Teukolsky, W. T. Vetterling, *Numerical recipes in C: The art of scientific computing*, 2nd edn., Cambridge University Press, Cambridge, **1993**.

